Kinetics of Mutant Apomyoglobin Association

Natalya Katina,[1] *Alexander Timchenko,*[1] *Hiroshi Kihara,*[2] *Vitaly Balobanov,*[1] *Victor Vasiliev,*[1] *Ivan Kashparov,*[1] *Valentina Bychkova**[1]

Summary: Association of protein molecules in human tissues underlies many diseases, which brings it in the focus of numerous studies. Previous reports described amyloid formation with the unfolded protein state taken as the starting point. Here, we present kinetics of protein aggregation starting from the protein native state and with consideration of its structural stability. We constructed mutant forms of apomyoglobin (apoMb) and investigated them by light scattering, small-angle X-ray scattering (SAXS), transmission electron microscopy (TEM), atomic force microscopy (AFM), fluorescence, far UV CD and FTIR spectroscopy. We found that apoMb mutants formed aggregates that changed their shape after 24 h incubation at a physiologically relevant temperature of 40 °C, pH 5.5, from almost globular (micellar) to elongated and curly. The elongated particles exhibited properties of the cross-beta structure characteristic of amyloids. According to SAXS, the elongated aggregates were not less than 300 Å in length, the gyration radius of their cross-section (R_c) was about 35 Å, and their molecular mass was over 400 kDa. An elongated shape of the aggregates was also demonstrated by TEM- and AFM imaging. The ability of apoMb mutants to form elongated amyloid-like aggregates, as well as their compactness, negatively correlated with stability of their native structure.

Keywords: aggregation kinetics; amyloids; apomyoglobin mutants; protein association; SAXS

Introduction

Many human diseases are connected with incorrect protein folding (or misfolding) due to biosynthesis errors and/or possible changes in the cell cycle.[1] Such proteins may form aggregates in the cell, which, in turn, can interfere with some cellular events like translocation, differentiation, intracellular transport, etc.[2] Studies of the process of protein association and investigation of protein aggregates by various techniques are therefore very important. Substantial progress in understanding of amyloid formation was achieved during the last decade.[3–5] However, there are few reports on time-dependent structural changes occurring in protein aggregates during their formation.[6–9] It should be emphasized that many studies were performed under denaturing conditions, and only some of them used native-like conditions similar to those existing in the cell.[9–11] This work was aimed to study kinetics of protein aggregation by a variety of techniques and the relationship between structural protein stability and the ability to form amyloids. Light scattering, SAXS, TEM and AFM, as well as more traditional far UV CD and FTIR spectroscopy and fluorescence were used for this purpose under nearly cellular conditions. Model proteins for amyloid formation – apoMb mutants with Ala and Trp substituted for Met131, and Val10Phe – were incubated for 24 h at an almost physiologically relevant (for a human body) temperature of 40 °C. At this temperature

[1] Institute of Protein Research, Russian Academy of Sciences, 4 Institutskaya St., 142290 Pushchino, Moscow Region, Russian Federation
Fax: (+7) 4967 318435;
E-mail: bychkova@vega.protres.ru
[2] Department of Physics, Kansai Medical University, Uyama-Higashi, Hirakata 573-1136, Osaka, Japan

the native states of the apoMb mutants (corresponding to those shown on the base lines of their temperature- and pH-induced denaturation transitions) were preserved. Thus, unlike in other studies, here the starting point of monitoring of protein association was the folded protein structure instead of its unfolded state. It was shown that these mutants were able to form amyloid-like structures after incubation in native-like conditions for a long time. SAXS showed that aggregates formed by different mutants differed in the number of monomers and type of their packing. No other technique but SAXS could give these results. It was also shown that curly amyloid protofibrils contained straight regions that were at least 300 Å long, which is the limiting value accessible for the used SAXS configuration. The calculated diameter of protofibrils was close to that estimated from TEM images.

Materials and Methods

Protein Expression and Isolation

ApoMb WT and its mutants (Met131Ala, Met131Trp, Val10Phe) were isolated after expression of the appropriate plasmids in *E. coli* BL21 (DE3) cells.[12,13] Cells were lysed using lysozyme, and proteins were purified from inclusion bodies by reversed-phase chromatography as previously described.[12] The lyophilized protein was checked for purity by SDS gel electrophoresis.

Measuring Conditions

Lyophilized proteins were dissolved to a final concentration of 5 mg/ml in milli-Q water-based 10 mM Na-phosphate buffer without any salt, pH 5.5, to be used in all experiments. If a particular technique required a lower protein concentration, an aliquot was taken and diluted with the buffer for every point. Prior to aggregation experiments, the samples of protein solution were centrifuged at 70,000 rpm for 30 min at 4 °C using a Beckman 100 ultracentrifuge with a TLA 100 rotor. The process of amyloid formation was studied by incubating the protein samples at 40 °C for various time intervals. The protein concentration was determined by spectrophotometric method (Cary 100, Australia) at 280 nm. The extinction coefficient was found by the nitrogen micromethod[14] as $A^{1cm}{}_{1mg/ml} = 0.88$ both for apoMb WT and its Met131Ala- and Val10Phe mutants, and 1.22 for the Met131Trp mutant.[13]

FTIR Spectroscopy

A Nicolet 6700 Fourier transform spectrometer (Thermo Scientific, USA) was used to measure FTIR spectra at 27 °C. The protein concentration was 5 mg/ml. The samples were placed between CaF_2 plates; the optical path length was 5.8 μm. Each spectrum, an average of 256 scanning results, was taken at a resolution of 4 cm^{-1}; in the course of measurement, water vapor spectra were automatically suppressed. The band typical of a cross-beta structure in the absorption spectrum located near 1620 cm^{-1} and that typical of an alpha-helical structure – near 1650 cm^{-1}.[15]

Fluorescence and Light Scattering

A Varian Cary Eclipse (Australia) spectrofluorimeter was used for Thioflavin T (ThT) fluorescence and light scattering registration. ThT fluorescence spectra were recorded at the 450 nm excitation wavelength and 20 °C over a range of 460–600 nm. In the studied samples, the protein concentration was 0.5 mg/ml, and that of dye was 4 μM. The kinetic curves were plotted with ThT fluorescence intensity recorded at 480 nm.

In light scattering experiments, the protein concentration was 0.1 mg/ml, the excitation wavelength was 600 nm, and the recorded spectra were within the 590–690 nm range.

Circular Dichroism

A JASCO J-600 (Japan) spectropolarimeter with 0.1-mm path length cells was used to obtain CD spectra and denaturation

curves. The protein concentration was 1 mg/ml. The molar ellipticity parameter *[θ]* was derived from $[\theta] = \theta \cdot MRW/l \cdot c$, where θ is its measured value (deg, 10^{-3}), MRW is the average residue molecular weight calculated from the amino acid sequence, l is the path length, and c is the protein concentration (mg/ml). Changes in far UV CD spectra upon aggregation were detected by ratio between intensities at 215 and 222 nm. The denaturation curves caused by decreasing pH were monitored through ellipticity changes at 222 nm.

Transmission Electron Microscopy (TEM)

The samples were negatively stained with 1% aqueous uranyl acetate using the single-layer carbon technique.[16] Carbon films (2–3 nm thick) on the surface of freshly cleaved mica were prepared using an electron beam evaporator.[17] Electron micrographs were taken using a JEM-100C electron microscope (JEOL, Japan) at an accelerating voltage of 80 kV and magnification of 40,000. The protein concentration was 0.1–0.05 mg/ml.

AFM

For AFM study, protein solution (5 mg/ml) was incubated at 40 °C and cooled after a fixed time interval. An aliquot of the protein sample (after dilution up to 1 ng/μl with pH 5.5 buffer) was applied onto a freshly cleaved mica plate. After 3 min-long aggregate sorption, the mica was rinsed three times with 200 μl of milli-Q water and dried under vacuum for 3 h before scanning by AFM. The AFM images were obtained using a FemtoScan Multi-Mode instrument (FemtoScan, Russia) operating in a contact mode.

Small Angle X-Ray Scattering (SAXS)

All SAXS experiments were carried out using a small-angle BL-15A camera of Photon Factory (Tsukuba, Japan).[18] The protein solution in a temperature-controlled cell with mica windows (V~30 μl) was irradiated by X-rays with $\lambda = 1.503$ Å wavelength at room temperature. The data registration was provided by a 2D CCD X-ray detector. The results were corrected for image distortion, nonlinear response and contrast. The sample-detector distance was 1.83 m, and the range of scattering vectors Q was 0.01–0.2 $Å^{-1}$(where $Q = 4\pi\sin\theta/\lambda$ and 2θ is the scattering angle). To find molecular masses of the studied proteins from the initial ordinate of the scattering curve, a measurement of bovine serum albumin (BSA) with the known molecular mass and dimensions was performed. The SAXS patterns were treated using SAXTIM and SIGMA PLOT 2000. The protein concentration used for SAXS measurements was 5.0 mg/ml. The apoMb samples were in 10 mM Na-P buffer, pH 5.5. To avoid aggregation upon X-rays irradiation, several short scans were made and checked separately.

The SAXS technique permits studying the overall shape, dimension and oligomeric state of macromolecules in solution. At very small scattering angles the Guinier approximation of scattering intensity I(Q) is valid: $I(Q) = I(0)^{*}\exp(-(Q^{*}R_g)^2/3)$, where R_g is the radius of gyration of a particle.[19] The Guinier plot represents the dependence of log I on Q^2 and permits estimating molecular masses of scattering particles (from the initial ordinate) and their average dimensions (from the initial slope of scattering curves). In the case of elongated particles the dependence $Q^{*}I(Q) = I_c(0)^{*}\exp(-(Q^{*}R_c)^2/2)$ is valid permitting to find the radius of gyration of cross-section R_c. At higher scattering angles where the overall shape of a particle essentially contributes to the scattering curve one can approximately describe this shape by plotting SAXS patterns in coordinates $I^{*}Q^2$ *vs* Q (the so-called Kratky plot). A maximum on this plot reflects a compact state, a straight line – an elongated one, and a plateau – a coiled one or a plane conformation.

Aggregation kinetics Assay

The kinetics of aggregate formation was studied through varying ThT fluorescence data and far UV CD spectra, AFM and TEM-controlled particle growth. In kinetic

experiments on ThT fluorescence and light scattering, the final protein concentration was 5 mg/ml, and the final ThT concentration was 40 μM. To monitor aggregation kinetics by far UV CD, aliquots of protein solution were sampled after various incubation intervals, far UV CD spectra were recorded, and the ratios of ellipticity at 215 and 222 nm were plotted *vs* time.

Results and Disscussion

Comparison of Properties of the Studied Proteins before and after 24 h Incubation

A 24 h incubation of apoMb mutants at 40 °C leads to changes in their properties. Their initially monomeric structure transforms into aggregates, which may be accompanied by increased light scattering intensity and enhanced ThT fluorescence intensity. These results are presented in Figure 1. Changes in light scattering intensity for Met131Trp mutant are shown in Inset to Figure 1c. A similar increase in light scattering intensity was characteristic of all the studied proteins (apoMb WT, apoMb Val10Phe, and apoMb Met131Ala) after 24 h incubation, which is indicative of aggregate formation in the protein solutions.

It is well known that apoMb WT is an alpha-helical protein. To observe changes in its secondary structure upon aggregation, FTIR spectroscopy was used, because it is this technique that, due to its insensitivity to aggregation, allows detecting the beta- or cross-beta secondary structure in proteins. Changes occurring in the secondary structure of apoMb mutants after 24 h incubation at 40 °C can be seen in Figure 2.

In Figure 2, the post-incubation FTIR spectra show a distinct band around 1620 cm^{-1}. As known, this is characteristic of the aggregated cross-beta structure, while the beta-structure is usually located around 1630 cm^{-1} (the positions of 1620 and 1630 cm^{-1} are shown by vertical lines). Estimates of the maximum positions were also found by plotting the second derivatives of FTIR spectra (not shown). This means that apoMb mutants form specific amyloid-like aggregates. FTIR spectra for the Met131Trp mutant are very close to those of apoMb WT (see below). Similar FTIR spectra for horse heart apoMb were reported previously as well as for lysozyme and insulin.[20–22] These aggregates have a curly elongated morphology and their length can reach 1000 Å as seen from TEM images (Figure 3).

For comparison, the equilibrium data on apoMb WT in monomeric and aggregated forms are presented in Figure 4.

Nothing but light scattering spectra of apoMb WT shows significant changes. The TEM image demonstrates that apoMb WT aggregates are less abundant than those formed by the mutants. Both far UV CD spectra of apoMb WT are very close to each other, which, together with minor changes in ThT fluorescence intensity, allow suggesting the presence of rather non-specific aggregates at this temperature.

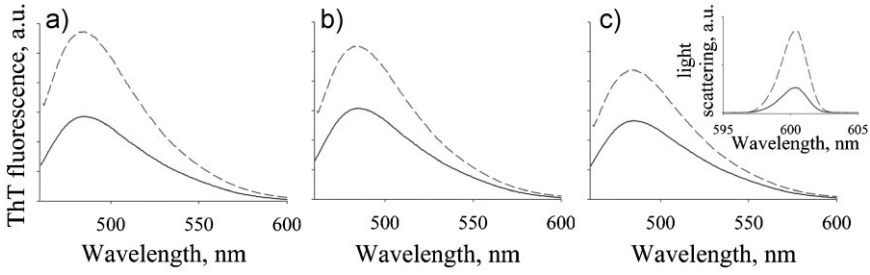

Figure 1.
Changes in ThT fluorescence spectra. Spectra for monomeric proteins before incubation are shown as solid lines, and spectra for aggregated proteins (after 24 h incubation) as dashed lines: a) Val10Phe; b) Met131Ala; c) Met131Trp (*Inset*: light scattering data for the same mutant form).

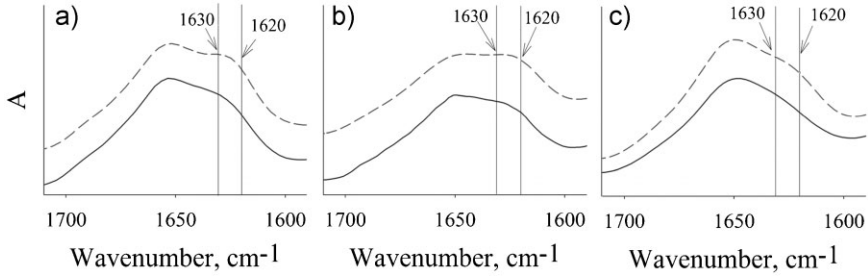

Figure 2.
FTIR spectra (*A*, absorption in arbitrary units) of the studied apoMb mutants before and after 24 h incubation at 40 °C: a) Val10Phe; b) Met131Ala; c) Met131Trp. Spectra for monomeric forms are shown as solid lines, and those for aggregated forms after 24 h incubation as dashed lines.

Stability of the studied proteins was taken as a pH value which corresponds to the middle of pH-induced transition from the native to intermediate state monitored by changes in intensity at 222 nm in far UV CD spectra presented in Figure 5 (see also[9]).

As it follows from Figure 5, for Val10Phe and Met131Ala, the middle of pH-induced transition is substantially shifted to higher pH values in comparison with Met131Trp that behaves like apoMb WT. This shift is evidence for decreased stability of these two mutants as compared to Met131Trp (and also to apoMb WT).

Small Angle X-Ray Scattering (SAXS)

SAXS is a powerful method to study conformations of particles in solution. SAXS patterns for the three apoMb mutants in coordinates log I^*Q *vs* Q^2 are presented in Figure 6. The same patterns in the Guinier coordinates (log I *vs* Q^2) are shown in *Inset* to Figure 6. By plotting log $(Q^*I(Q))$ *vs* Q^2 one can evaluate the radius of gyration of the cross-section (R_c) (for a uniform cylindrical particle, R_c is $\sqrt{}$2-times less than its radius). From the slope of experimental curves R_c value can be calculated. Obtained R_c values for Met131Trp, Val10Phe, Met131Ala are equal to 30.2 Å, 33.0 Å, and 33.4 Å, respectively. Taking R_c into account, it is possible to calculate the length L of a uniform scattering particle from: $L = \sqrt{}12 *(R_g^2 - R_c^2)$. The estimated L values for the same mutant apoMbs are 315 Å, 350 Å, 350 Å, respectively. It is known that such estimation is correct within the $2\pi/L < Q < 1/R_c$ range of scattering vectors, which is true in our case.[23]

The Guinier plots for all the mutants are presented in *Inset* to Figure 6. One can see the essential non-linear character of scat-

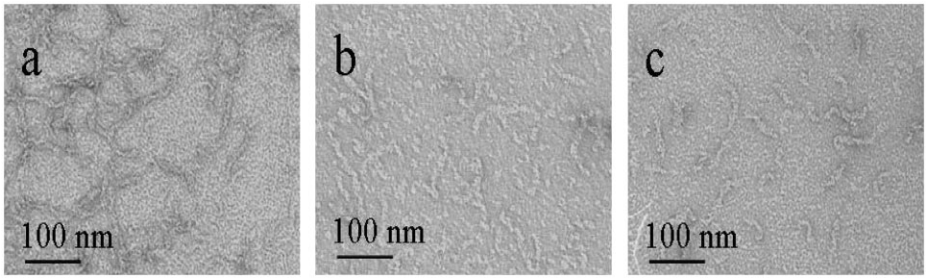

Figure 3.
Electron microscopy images of aggregates formed by apoMb mutants after 24 h incubation at 40 °C: a) Val10Phe; b) Met131Ala; c) Met131Trp.

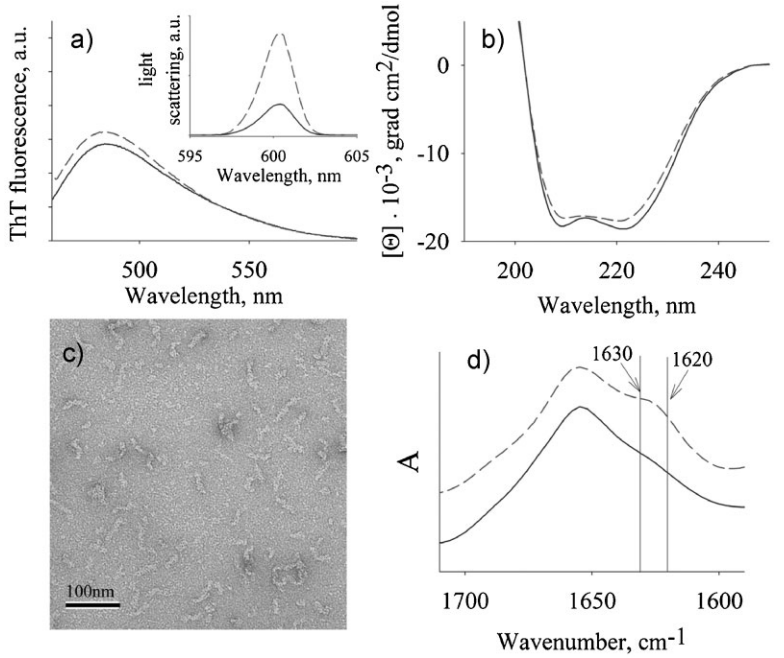

Figure 4.
Comparison of the properties of apoMb WT before incubation with those of its aggregates formed after 24 h incubation at 40 °C, pH 5.5. *a*) ThT fluorescence spectra (*Inset*: light scattering spectra at 600 nm); b) far UV CD spectra; *c*) TEM image of the aggregates; d) FTIR spectra; spectra for apoMb WT before incubation are shown as solid lines, and those for the aggregates after 24 h incubation at 40 °C as dashed lines.

tering curves indicating substantial association of protein molecules. The values of molecular masses (M_w) and gyration radii (R_g) of particles estimated from the initial part of scattering curves are given in the legend to Figure 6. These estimates show significant association of the apoMb mutants. A lower M_w (400 kDa) and a slightly higher R_g (96 Å) for Met131Trp, as compared with those of the other mutants (620–770 kDa and 92–107 Å), point to a less compact packing of its aggregates. It should be emphasized that this mutant has a more stable native structure comparable to that of apoMb WT, and probably this is the reason why it forms less compact aggregates containing a lower number of monomers with M_w 17 kDa.

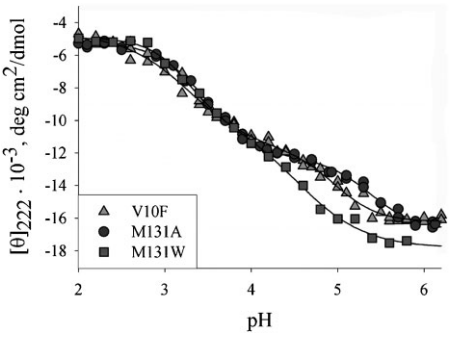

Figure 5.
Dependence of molar ellipticity on pH for Val10Phe (▲), Met131Ala (●), and Met131Trp (■).

The major contribution of the associates to the scattering pattern is observed in its initial part. Then it is possible to describe approximate shapes of these aggregates by plotting log I *versus* log Q (not shown) and finding the slopes of these dependences. As estimated, the slopes range from −1.3 to −1.1, which is close to −1.0, that is characteristic of strongly elongated particles (these linear regions on the Kratky plot are shown in *Inset* to Figure 8, see below). This fact indicates that these aggregates have a strongly elongated shape, which is in

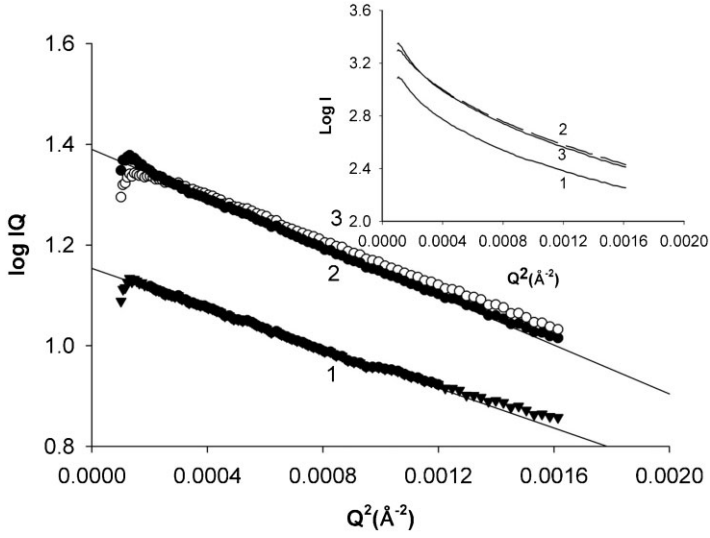

Figure 6.
Log IQ *vs* Q^2 plot of scattering patterns for evaluation of R_c for apoMb mutants: 1 - Met131Trp, 2 - Val10Phe, 3 - Met131Ala. *Inset*: The Guinier plots of scattering patterns. Molecular masses and gyration radii evaluated from the initial part of scattering patterns: $M_w = 400$ kDa, 620 kDa, 770 kDa; $R_g = 96$ Å, 92 Å, 107 Å, respectively.

agreement with TEM data (see Figure 3). For such asymmetric particles, it is possible to get additional information on their structure. It is known that for strongly elongated particles the accuracy of R_g estimates is not high. Therefore, we evaluated the errors for R_g and L by the model calculation for a system with linear configuration of spheres ($R = 50$ Å) having the same R_c as estimated from the experiment. The Guinier plot for such a system is presented in Figure 7, where R_g evaluation was made in the same region of scattering vector as for experimental scattering curves (0.01–0.014 $Å^{-1}$). For a model of three spheres in line the estimate for R_g differs from the theoretical one by no more than 5%, and for L the difference does not exceed 8%. One can see from Figure 7 that longer particles do not contribute much to the experimental Q region. Therefore, the estimated value of L equal to about 300 Å can be taken as a limiting L value for our experimental conditions.

At higher scattering angles more details of a scattering particle structure are seen. In Figure 8 the Kratky plots of SAXS patterns of all the studied apoMb forms over the entire experimental range of Q values are presented.[19] As seen, the scattering curves for Met131Ala and Val10Phe are well bell-shaped, which is characteristic of a compact particle organization. R_g can be evaluated from the maximum position using the equation $R_g = \mathrm{sqrt}(3)/Q_{max}$.[24] Its estimated value of 45 Å corresponds to globular aggregates of monomers comprising elongated protofibrils (particles).

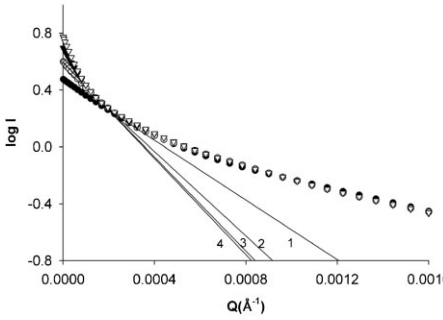

Figure 7.
The Guinier plots of SAXS patterns from the model system of linear configuration of spheres ($R = 50$ Å). Regression lines are (1) for three spheres (•), (2) – four spheres (○), (3) – five spheres (▼), (4) – six spheres (△).

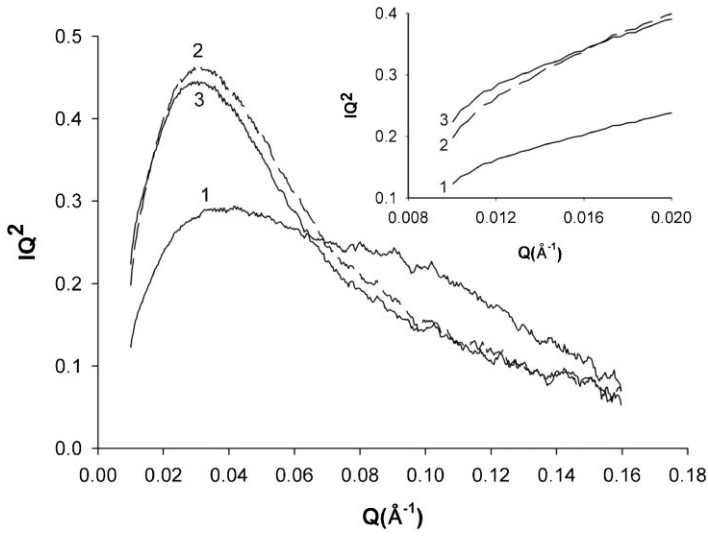

Figure 8.
The Kratky plots of SAXS patterns for the same mutants as in Figure 6: 1, Met131Trp; 2, Val10Phe; 3, Met131Ala. *Inset*: initial parts of all Kratky plots.

It should be noted that the scattering particles have different M_W (400 kDa for Met131Trp and 620–770 kDa for the others) but a similar R_g of 90–100 Å, as seen from Figure 6. This means that the aggregates formed by Met131Trp incorporate only half of monomer units as compared with the others. Moreover, for this mutant a long decay of the Kratky plot is observed. All these peculiarities in behavior of Met131Trp reflect a more loose packing of monomers incorporated in its elongated 400 kDa aggregates. Also, it has a more stable native structure in the monomeric form than other mutants. *Inset* to Figure 8 presents the initial parts of the Kratky plots at small scattering angles to demonstrate behavior of the whole elongated aggregates. As seen, at these angles linear dependences are observed. This proves the presence of strongly elongated particles in solution after 24 h incubation at 40 °C.

Kinetics of Association of ApoMb Mutants

Kinetics of protein aggregation was monitored by increasing intensity of ThT fluorescence, AFM, TEM and SAXS (the Kratky plots), as presented below. Incubation of protein solutions (5 mg/ml) at 40 °C leads to changes in their properties observed by a variety of methods. It should be stressed that under conditions of pH 5.5 and 40 °C the structures of the studied mutants corresponded to their compact native states, as seen on the base lines of their pH- and temperature-induced transitions. The increasing light scattering intensity reflected increasing dimensions of protein aggregates. On the other hand, the increasing intensity of ThT fluorescence was indicative of formation of the cross-beta structure in growing aggregates, as opposed to monomeric apoMb having solely the alpha-helical secondary structure. These data are presented in Figure 9.

Incubation time-dependent changes in morphology of formed apoMb Val10Phe aggregates monitored by AFM and TEM are shown in Figure 10 and 11.

The both techniques show growth of aggregates with time. The diversity in dimensions is observed up to 11 h (see Figure 11). Small globular (micellar) aggregates could be seen after any incubation period (no significant changes were

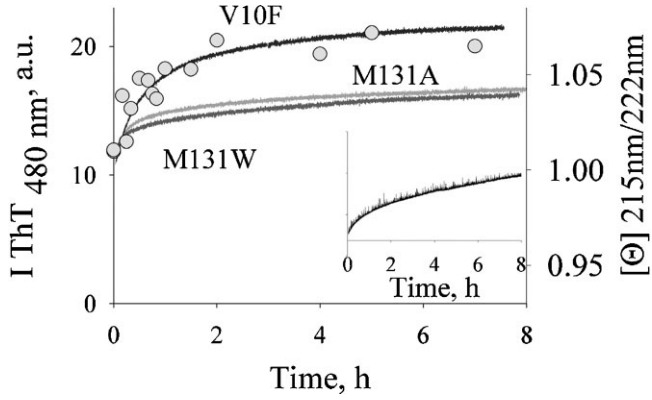

Figure 9.
Time-dependence of ThT fluorescence intensity at 40 °C for apoMb Val10Phe, apoMb Met131Ala, and apoMb Met131Trp. *Inset*: Changes in light scattering intensity at 600 nm (A) for apoMb Val10Phe. Similar dependences were observed for other apoMb mutants. Circles near the curve for Val10Phe reflect the changing ratio between intensities at 215 and 222 nm in their far UV CD spectra (a scale is shown on the right).

observed until 10 days of incubation). It is quite plausible that the growth of protofibrils might occur via attaching these globular aggregates to the growing fibril end. The protofibrils can be as large as 1000 Å in length, and their diameter estimate is about 100 Å.

The SAXS technique is most useful in detecting changes in particles with slow kinetics. Figure 12 presents the Kratky plots of SAXS patterns of amyloid formation kinetics. An increase in scattering intensity and overall dimensions is clearly observed during 80 min. Then, the formed aggregates show almost no changes, and the maximum position shifts only slightly, which is indicative of compact packing of the monomers in globular aggregates over the entire process (aggregation process started from the compact state of the protein). *Inset* to Figure 12

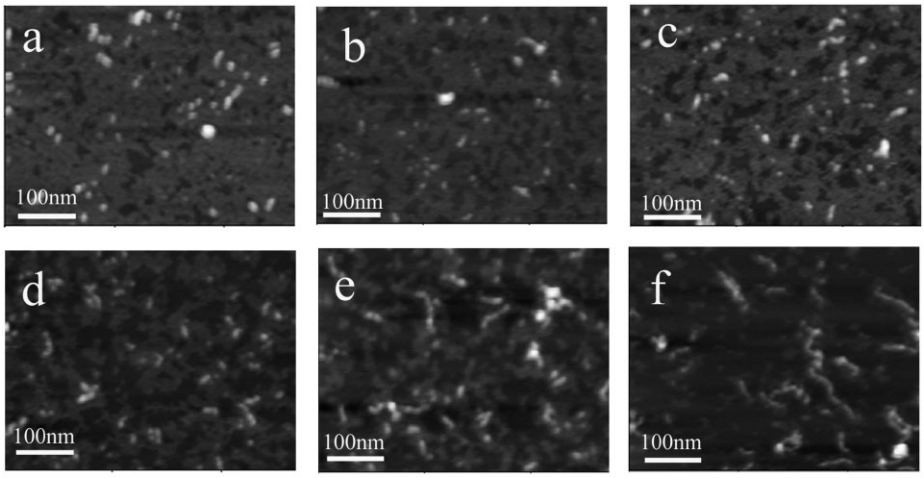

Figure 10.
Kinetics of apoMb Val10Phe aggregate formation monitored by AFM after incubation at 40 °C for: a) 10 min; b) 20 min; c) 1 h; d) 2 h; e) 6 h; f) 24 h.

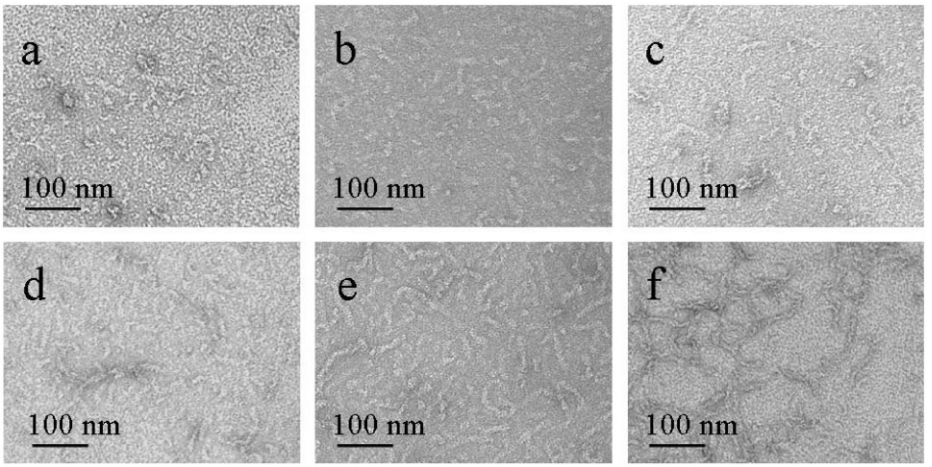

Figure 11.
TEM images of aggregates formed by apoMb Val10Phe mutant after incubation at 40 °C for: a) 20 min; b) 40 min; c) 1.5 h; d) 6 h; e) 11 h; f) 24 h.

presents changes occurring with time in the calculated R_g value for particles.

A R_g drop during the initial minutes is clearly seen. This effect was unexpected. It is possible that immediately after heating to 40 °C nonspecific aggregates formed in the course of sample preparation were disrupted. This could explain the decreased aggregate dimensions. Further incubation at 40 °C could give rise to formation of more specific aggregates. After 20 min incubation an increase in R_g value is clearly seen,

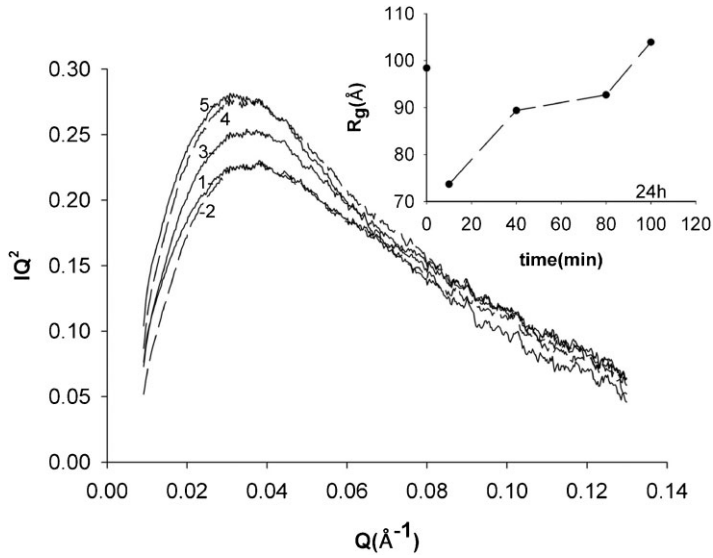

Figure 12.
Measured scattering patterns are presented as the Kratky plots for apoMb Val10Phe subjected to incubation at 40 °C, pH 5.5, for: 1) 0 min (just after heating to 40 °C), 2) 10 min, 3) 40 min, 4) 80 min, 5) 24 h. *Inset*: time dependence of R_g.

which indicates that the particle dimensions increased with incubation time.

Taken together, the above results are convincing evidence for formation of amyloid-like aggregates by the apoMb mutants proved by ThT fluorescence, FTIR, TEM and AFM. SAXS was most useful to demonstrate that aggregates formed by different mutants differed in the number of associated monomers and in the type of their packing. It was also shown that curly amyloid protofibrils contained straight regions that were at least 300 Å long, which is the limiting value for a SAXS BL-15A installation. The calculated diameter of protofibrils (~100 Å) was close to that estimated from TEM images.

Of note, a structural description of fibril formation using SAXS has been reported in a few papers only. Similar results were obtained by other research teams for different proteins. A very detailed SAXS study was performed on glucagon fibrillation.[25] The authors described formation of obligatory on-pathway early oligomers before appearance of mature fibrils. The mechanism of amyloid protofibril formation by barstar was in the focus of another study that revealed its multistep nature, as well as a conformational conversion within the aggregates at late steps of their assembly into protofibrils.[26] Characterization of the initial stage of fibril formation by another protein, alpha-synuclein, has been performed using SAXS, NMR and TEM.[27] A variety of techniques for structural characterization of prefibrillar intermediates and mature amyloids have been recently reviewed.[28] Our data are in agreement with literature data and support appearance of oligomers on earlier stages of aggregation process.

Conclusion

Kinetics of mutant apoMb aggregation and amyloid formation was monitored by changing the ThT fluorescence intensity, TEM, AFM, and SAXS. All these techniques show formation of aggregates of different size and shape, depending on incubation time. The SAXS-estimated length of scattering particles L of about 300 Å can be taken as the limiting L value for the applied resolution. At the same time, by TEM the protofibril length was up to 1000 Å. These particles were characterized by an increased molecular mass and had R_c of about 35Å and R_g of approximately 100Å, as shown by SAXS. An elongated shape of apoMb aggregates was proved by TEM, SAXS, and AFM. Diameters of the particles given by TEM and SAXS were in good agreement. An ability of apoMb mutants to form elongated aggregates and compactness of these aggregates negatively correlate with stability of their native structures: the higher stability, the lower amyloid formation ability. During the first two hours of incubation, globular aggregates were predominant, although a small number of elongated particles were also observed. After 6 h incubation elongated curved protofibrils dominated. Nevertheless, globular aggregates were still observed until 24 h incubation. This allows suggesting that elongation of the curved fibrils occurred through attachment of these globular aggregates to the growing fibril end. Probably, the main puzzle of amyloid formation is transformation of early aggregates into fibrils, especially if an initially helical protein (like apoMb) attains the fibrillar configuration with the cross-beta secondary structure simply as a result of its incubation under native-like conditions for a long time. However, additional experiments are required to understand at what stage the apoMb alpha-helical structure partially transforms into the cross-beta one.

Acknowledgements: The study was supported by the Program on ''Molecular and Cell Biology'' and ''Leading Scientific Schools'' from the Presidium of Russian Academy of Sciences, and by grants from the Russian Foundation for Basic Research, the Federal Science and Innovation Agency, and Howard Hughes Medical Institute to A.V. Finkelstein. This study was approved by the Photon Factory (Proposal No. 2007G645). The authors are grateful to N.B.

Ilyina and A.A. Bogdanov for help in measurements.

[1] F. Chiti, C. M. Dobson, *Annu. Rev. Biochem.* **2006**, *75*, 333.
[2] E. Herczenik, M. F. B. G. Gebbink, *The FASEB J.* **2008**, *22*, 2115.
[3] H. E. White, J. L. Hodgkinson, T. R. Jahn, S. Cohen-Klausz, W. S. Gosal, S. Mueller, E. V. Orlova, S. E. Radford, H. R. Saibil, *J. Mol. Biol.* **2009**, *389*, 48.
[4] F. Chiti, C. M. Dobson, *Nature Chem. Biol.* **2009**, *5*, 15.
[5] T. M. Ryan, C. L. Teoh, M. D. W. Griffin, M. F. Bailey, P. Schuck, G. J. Howlett, *J. Mol. Biol.* **2010**, *399*, 731.
[6] D. P. Smith, S. Jones, L. C. Serpell, M. Sunde, S. E. Radford, *J. Mol. Biol.* **2003**, *330*, 943.
[7] A. J. Molder, K. Gast, G. Lutsch, G. Damaschun, *J. Mol. Biol.* **2003**, *325*, 135.
[8] J. Kaylor, N. Bodner, S. Edridge, G. Yamin, D.-P. Hong, A. L. Fink, *J. Mol. Biol.* **2005**, *353*, 357.
[9] N. S. Katina, N. B. Ilyina, I. A. Kashparov, V. A. Balobanov, V. D. Vasiliev, V. E. Bychkova, *Biochemistry (Moscow)* **2011**, *76*, 680 (*Russian version*), (555 for *English version*).
[10] F. Bemporad, F. Chiti, *FEBS Lett.* **2009**, *583*, 2630.
[11] G. Soldi, F. Bemporad, S. Torrassa, A. Relini, M. Ramazzotti, N. Taddei, F. Chiti, *Biophys. J.* **2005**, *89*, 4234.
[12] P. A. Jennings, M. J. Stone, P. E. Wright, *J. Biomol. NMR* **1995**, *6*, 271.
[13] A. E. Dyuysekina, D. A. Dolgikh, E. N. Samatova (Baryshnikova), E. I. Tiktopulo, V. A. Balobanov, V. E. Bychkova, *Biochemistry (Moscow)* **2008**, *73*, 863.
[14] L. Jaenicke, *Anal. Biochem.* **1974**, *61*, 623.
[15] J. Kong, S. Yu, *Acta Biochim. Biophys. Sin. (Shanghai)* **2007**, *39*, 549.
[16] R. C. Valentine, B. M. Shapiro, E. R. Stadtman, *Biochemistry* **1968**, *7*, 2143.
[17] V. D. Vasiliev, V. E. Koteliansky, *Methods Enzymol.* **1979**, *59*, 612.
[18] Y. Amemiya, K. Wakabayashi, T. Hamanaka, T. Wakabayashi, T. Matsushima, H. Hashizume, *Nucl. Instr. Methods* **1983**, *208*, 471.
[19] O. Glatter, O. Kratky, in: "*Small Angle X-ray Scattering*", Academic Press, London **1982**, p. 1–515.
[20] M. R. H. Krebs, G. L. Devlin, A. M. Donald, *Biophys. J.* **2007**, *92*, 1336.
[21] M. F. Mossuto, A. Dhulesia, G. Devlin, E. Frare, J. R. Kumita, P. Polverino, M. de Laureto Dumoulin, A. Fontana, C. M. Dobson, X. Salvatella, *J. Mol. Biol.* **2010**, *402*, 783.
[22] R. Maeda, K. Ado, N. Takeda, Y. Taniguchi, *Biochem. Biophys. Acta* **2007**, *1774*, 1619.
[23] L. A. Feigin, D. I. Svergun, in: "*Structure Analysis by Small-Angle X-Ray and Neutron Scattering*", Plenum Press, New York **1987**, pp. 335.
[24] G. V. Semisotnov, H. Kihara, N. V. Kotova, K. Kimura, Y. Amemiya, K. Wakabayashi, I. N. Serdyuk, A. A. Timchenko, K. Chiba, K. Nikaido, T. Ikura, K. Kuwajima, *J. Mol. Biol.* **1996**, *262*, 559.
[25] C. L. P. Olivera, M. A. Behrens, J. S. Pedersen, K. Erlacher, D. Otzen, J. S. Pedersen, *J. Mol. Biol.* **2009**, *387*, 147.
[26] S. Kumar, S. K. Mohanty, J. B. Udgaonkar, *J. Mol. Biol.* **2007**, *367*, 1186.
[27] M. Tashiro, M. Kojima, H. Kihara, K. Kasai, T. Kamiyoshihara, K. Ueda, S. Shimotakahara, *Biochem. Biophys. Res. Commun.* **2008**, *369*, 910.
[28] A. E. Langkilde, B. Vestergaard, *FEBS Lett.* **2009**, *583*, 2600.

